Journal of Sound and Vibration (1998) **213**(4), 601–617

ACOUSTIC ATTENUATION PERFORMANCE OF CIRCULAR EXPANSION CHAMBERS WITH OFFSET INLET/OUTLET: I. ANALYTICAL APPROACH

A. SELAMET AND Z. L. JI

Department of Mechanical Engineering and The Centre for Automotive Research, The Ohio State University, Columbus, OH 43210-1107, *U.S.A.*

(*Received* 20 *August* 1997, *and in final form* 8 *January* 1998)

The inlet and outlet locations of expansion chambers can significantly affect the acoustic attenuation performance of the silencer, due to their control over the excitation and suppression of higher order modes. By combining the continuity conditions of the acoustic pressure and particle velocity with the orthogonality relations of Fourier–Bessel functions at the inlet and outlet discontinuities, the present study develops a three-dimensional analytical approach to determine the transmission loss of circular expansion chambers with offset inlet and outlet ducts. The results obtained from the present approach are compared with the classical one-dimensional predictions and the earlier multidimensional works.

1. INTRODUCTION

The expansion chamber is a common and desirable silencer in pulsating internal flows due to its usually broad band(s) of acoustic attenuation. By assuming linear waves in a stationary medium, Davis *et al*. [1] were the first to introduce a one-dimensional analytical approach for the expansion chamber. The resulting closed-form expression for transmission loss was a function of the area expansion ratio and the dimensionless frequency parameter kl with a periodicity of π, k being the wavenumber and l the chamber length. This useful attempt of Davis *et al*., however, excludes wave propagation in the transverse direction and, therefore, the higher order modes which are generated at the area discontinuities at the inlet and outlet of the chamber. For particularly short-length expansion chambers, some evanescent modes excited at these discontinuities may not decay sufficiently within the chamber, and therefore affect the acoustic attenuation even in the low frequency region.

The multidimensional wave propagation due to area discontinuities is studied first by Miles [2]. Following the application of continuity boundary conditions for the acoustic pressure and particle velocity at the area discontinuities, Miles used the orthogonality relations of Bessel functions to develop a set of equations and then determined the incident and reflected waves. However, the work did not include either a numerical calculation or an experimental validation of the approach. El-Sharkawy and Nayfeh [3] later extended this work to a two-dimensional axisymmetric treatment of concentric expansion chambers, and also provided comparisons with the experimental noise reduction measurements for different expansion and length to diameter ratios. Utilizing the mode-matching technique, Åbom [4] derived the four-pole parameters that incorporated higher order mode effects in concentric expansion chambers with extended inlet and outlet. The computed transmission loss for a circular concentric configuration agreed well with the experiments.

Selamet and Radavich [5] investigated the effect of length on the acoustical attenuation performance of concentric expansion chambers, by using an analytical approach following Miles, a computational solution based on the boundary element method (BEM), and experiments on an extended impedance tube set-up. The results of all three approaches were shown to agree well. For a single asymmetric chamber, the same work also presented an experimental observation of the breakdown of one-dimensional behaviour at the first asymmetric mode (1, 0) rather than the first radial mode (0, 1) when the inlet and outlet locations were changed from concentric to offset. The foregoing studies represent the significant contributions to the understanding of primarily concentric expansion chambers.

Eriksson *et al*. [6–8] investigated experimentally the effect of inlet/outlet locations and the chamber length on the propagation of higher order modes in asymmetric expansion chambers. The offset distance, the offset angle for inlet/outlet locations, and the length of the chamber were found to have significant effects on the excitation, propagation, and suppression of the higher order modes. Ih and Lee [9] developed a three-dimensional analytical model for circular expansion chambers that incorporated mean flow and allowed for offset inlet and outlet locations. Their results matched the experimental transmission loss fairly well over a wide frequency range and for l/d ratios from 0·33 to 1·35. However, they chose to exclude the inlet and outlet ducts and modelled the chamber as a piston-driven circular rigid tube. The resulting analytical predictions in the absence of end ducts are expected to show some deviation from the experimental results (performed with the end ducts), particularly for larger offsets and shorter chambers due to the importance of decaying non-planar waves in the inlet and outlet ducts. Yi and Lee applied the same approach to circular expansion chambers with side-inlet/side-outlet and side-inlet/end-outlet [10, 11]. They also provided comparisons with the experimental results. By employing the eigenfunction expansion method, Kim and Soedel [12] studied the three-dimensional acoustic cavities and Lai and Soedel [13] the two-dimensional cavities, and derived the four-pole parameters. A limited number of asymmetric configurations with offset inlet and outlet has been studied recently in terms of BEM, and the importance of the effect of non-planar wave propagation in inlet and outlet ducts on the acoustic attentuation of expansion chambers has been demonstrated [14].

The objective of the present study is to develop *a three-dimensional analytical approach* to facilitate a detailed analysis of the effect of multidimensional wave propagation on the acoustic attenuation *in circular asymmetric expansion chambers with offset inlet and outlet ducts*. Following the Introduction, the analytical approach is described next. While some analytical results are presented and discussed subsequently, extensive comparisons with experiments and BEM are deferred to a companion work [15]. The study is concluded with some final remarks.

2. ANALYTICAL APPROACH

The three-dimensional sound propagation in a circular expansion chamber, as shown in Figure 1, is governed by the well-known Helmholtz equation [16]

$$\nabla^2 P + k^2 P = 0, \tag{1}$$

where P is the acoustic pressure, $k = \omega/c$ is the wavenumber, ω is the angular frequency, and c is the speed of sound. By employing the separation of variables, the solutions for

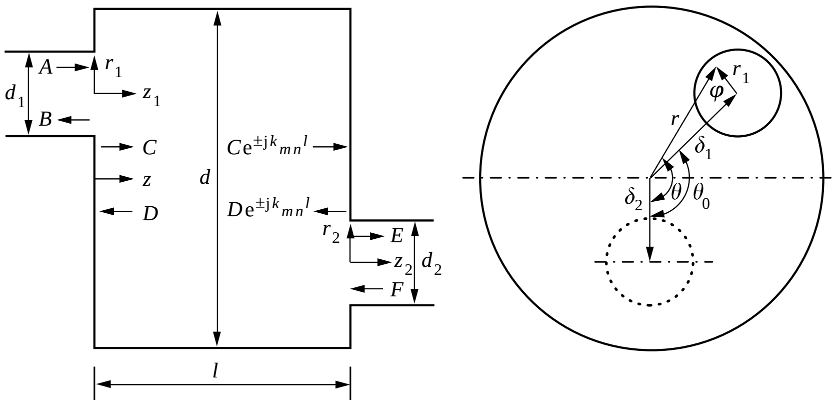

Figure 1. Asymmetric expansion chamber geometry: $d_1 = d_2 = 4{\cdot}859$ cm, $d = 15{\cdot}318$ cm, $\delta_1 = \delta_2 = 5{\cdot}10$ cm.

the acoustic pressure may be written, for a wave C travelling in the positive z-direction in a duct of radius a, as

$$P_C = C_{00}\,\mathrm{e}^{-\mathrm{j}kz} + \sum_{n=1}^{\infty} C_{0n}\mathrm{J}_0(\alpha_{0n}r/a)\,\mathrm{e}^{\mathrm{j}k_{0n}z}$$

$$+ \sum_{m=1}^{\infty}\sum_{n=0}^{\infty} (C_{mn}^{+}\,\mathrm{e}^{-\mathrm{j}m\theta} + C_{mn}^{-}\,\mathrm{e}^{\mathrm{j}m\theta})\mathrm{J}_m(\alpha_{mn}r/a)\,\mathrm{e}^{\mathrm{j}k_{mn}z}, \tag{2}$$

and, for a wave D travelling in the negative z-direction,

$$P_D = D_{00}\,\mathrm{e}^{\mathrm{j}kz} + \sum_{n=1}^{\infty} D_{0n}\mathrm{J}_0(\alpha_{0n}r/a)\,\mathrm{e}^{-\mathrm{j}k_{0n}z}$$

$$+ \sum_{m=1}^{\infty}\sum_{n=0}^{\infty} (D_{mn}^{+}\,\mathrm{e}^{-\mathrm{j}m\theta} + D_{mn}^{-}\,\mathrm{e}^{\mathrm{j}m\theta})\mathrm{J}_m(\alpha_{mn}r/a)\,\mathrm{e}^{-\mathrm{j}k_{mn}z}. \tag{3}$$

Here C and D are the complex pressure amplitudes of the waves travelling in the positive and negative z-directions, and the superscripts $+$ and $-$ designate the positive and negative θ-directions; $\mathrm{J}_m(x)$ is the Bessel function of the first kind of order m; α_{mn} is the root satisfying the radial boundary condition of

$$\mathrm{J}_m'(\alpha_{mn}) = 0, \tag{4}$$

TABLE 1

Roots, α_{mn}, of the Bessel function $\mathrm{J}_m'(\alpha_{mn}) = 0$

m/n	0	1	2	3	4	5
0	0·0	3·832	7·016	10·174	13·324	16·470
1	1·841	5·331	8·536	11·706	14·864	18·016
2	3·054	6·706	9·969	13·170	16·348	19·513
3	4·201	8·015	11·346	14·586	17·789	20·973
4	5·318	9·282	12·682	15·964	19·196	22·401
5	6·415	10·520	13·987	17·313	20·576	23·804

where m and n denote the asymmetric and radial mode numbers (see Table 1 for α_{mn}); and

$$k_{mn} = k[1 - (\alpha_{mn}/ka)^2]^{1/2}, \tag{5}$$

is the wavenumber of the mode (m, n). Examining equation (5) for any high order mode (m, n), k_{mn} will be imaginary when

$$f < \frac{c}{2\pi}\left(\frac{\alpha_{mn}}{a}\right). \tag{6}$$

The sign difference between the planar (0, 0) and higher order modes in the exponential terms of equations (2) and (3) ensures that for a wave travelling, for example, in the positive direction, the magnitude of all modes will decrease exponentially to zero with increasing distance when equation (6) is satisfied. The axial particle velocities for waves C and D are obtained from the momentum equation,

$$\mathrm{j}\rho\omega\mathbf{U} = -\nabla P, \tag{7}$$

as

$$U_C = \frac{1}{\rho\omega}\left\{kC_{00}\,\mathrm{e}^{-\mathrm{j}kz} - \sum_{n=1}^{\infty} k_{0n}C_{0n}\mathrm{J}_0(\alpha_{0n}r/a)\,\mathrm{e}^{\mathrm{j}k_{0n}z}\right.$$
$$\left. - \sum_{m=1}^{\infty}\sum_{n=0}^{\infty} k_{mn}(C^+_{mn}\,\mathrm{e}^{-\mathrm{j}m\theta} + C^-_{mn}\,\mathrm{e}^{\mathrm{j}m\theta})\mathrm{J}_m(\alpha_{mn}r/a)\,\mathrm{e}^{\mathrm{j}k_{mn}z}\right\} \tag{8}$$

and

$$U_D = -\frac{1}{\rho\omega}\left\{kD_{00}\,\mathrm{e}^{\mathrm{j}kz} - \sum_{n=1}^{\infty} k_{0n}D_{0n}\mathrm{J}_0(\alpha_{0n}r/a)\,\mathrm{e}^{-\mathrm{j}k_{0n}z}\right.$$
$$\left. - \sum_{m=1}^{\infty}\sum_{n=0}^{\infty} k_{mn}(D^+_{mn}\,\mathrm{e}^{-\mathrm{j}m\theta} + D^-_{mn}\,\mathrm{e}^{\mathrm{j}m\theta})\mathrm{J}_m(\alpha_{mn}r/a)\,\mathrm{e}^{-\mathrm{j}k_{mn}z}\right\}. \tag{9}$$

For the expansion chamber, equations (2) and (8) are used for waves A, C and E travelling in the positive z-direction, and equations (3) and (9) for waves B, D and F travelling in the negative z-direction (see Figure 1).

At the expansion, the boundary conditions reveal, for the pressure,

$$(P_A + P_B)|_{z_1=0} = (P_C + P_D)|_{z=0}, \qquad (\text{on } S_1), \tag{10}$$

and, for the velocity,

$$(U_A + U_B)|_{z_1=0} = (U_C + U_D)|_{z=0}, \qquad (\text{on } S_1); \qquad (U_C + U_D)|_{z=0} = 0, \qquad (\text{on } S - S_1), \tag{11, 12}$$

where S_1 and S are the cross-sectional areas of the inlet duct and the chamber, respectively. For the pressure boundary condition, multiply both sides of equation (10) by $J_t(\alpha_{ts} r_1/a_1)\, e^{jt\varphi}\, dS$ and integrate over S_1 to get, for $t = 0$ and $s = 0$,

$$[A_{00} + B_{00}]\frac{a_1^2}{2} = [C_{00} + D_{00}]\frac{a_1^2}{2} + \sum_{n=1}^{\infty}[C_{0n} + D_{0n}]\frac{aa_1}{\alpha_{0n}} J_0(\alpha_{0n}\delta_1/a)J_1(\alpha_{0n}a_1/a) + \sum_{m=1}^{\infty}\sum_{n=0}^{\infty}[(C_{mn}^{+} + D_{mn}^{+})\, e^{-jm\theta_0} + (C_{mn}^{-} + D_{mn}^{-})\, e^{jm\theta_0}] \times \frac{aa_1}{\alpha_{mn}} J_m(\alpha_{mn}\delta_1/a)J_1(\alpha_{mn}a_1/a), \tag{13}$$

for $t = 0$ and $s = 1, 2, \ldots, \infty$,

$$[A_{0s} + B_{0s}]\frac{a_1^2}{2} J_0(\alpha_{0s}) = \sum_{n=1}^{\infty}[C_{0n} + D_{0n}]J_0(\alpha_{0n}\delta_1/a)\frac{\alpha_{0n}a_1/aJ_0'(\alpha_{0n}a_1/a)}{(\alpha_{0s}/a_1)^2 - (\alpha_{0n}/a)^2} + \sum_{m=1}^{\infty}\sum_{n=0}^{\infty}[(C_{mn}^{+} + D_{mn}^{+})\, e^{-jm\theta_0} + (C_{mn}^{-} + D_{mn}^{-})\, e^{jm\theta_0}] \times J_m(\alpha_{mn}\delta_1/a)\frac{\alpha_{mn}a_1/aJ_0'(\alpha_{mn}a_1/a)}{(\alpha_{0s}/a_1)^2 - (\alpha_{mn}/a)^2}, \tag{14}$$

and for $t = 1, 2, \ldots, \infty$ and $s = 0, 1, \ldots, \infty$,

$$[A_{ts}^{+} + B_{ts}^{+}]\frac{a_1^2}{2}\left(1 - \frac{t^2}{\alpha_{ts}^2}\right)J_t(\alpha_{ts}) = \sum_{n=1}^{\infty}[C_{0n} + D_{0n}]J_t(\alpha_{0n}\delta_1/a)\frac{\alpha_{0n}a_1/aJ_t'(\alpha_{0n}a_1/a)}{(\alpha_{ts}/a_1)^2 - (\alpha_{0n}/a)^2} + \sum_{m=1}^{\infty}\sum_{n=0}^{\infty}[(C_{mn}^{+} + D_{mn}^{+})J_{m+t}(\alpha_{mn}\delta_1/a)\, e^{-jm\theta_0} + (C_{mn}^{-} + D_{mn}^{-})(-1)^t J_{m-t}(\alpha_{mn}\delta_1/a)\, e^{jm\theta_0}]\frac{\alpha_{mn}a_1/aJ_t'(\alpha_{mn}a_1/a)}{(\alpha_{ts}/a_1)^2 - (\alpha_{mn}/a)^2}. \tag{15}$$

Multiplying both sides of equation (10) by $J_t(\alpha_{ts} r_1/a_1)\, e^{-jt\varphi}\, dS$ and integrating over S_1, the following equation can be obtained, for $t = 1, 2, \ldots, \infty$ and $s = 0, 1, \ldots, \infty$,

$$[A_{ts}^{-} + B_{ts}^{-}]\frac{a_1^2}{2}\left(1 - \frac{t^2}{\alpha_{ts}^2}\right)J_t(\alpha_{ts}) = \sum_{n=1}^{\infty}[C_{0n} + D_{0n}]J_t(\alpha_{0n}\delta_1/a)\frac{\alpha_{0n}a_1/aJ_t'(\alpha_{0n}a_1/a)}{(\alpha_{ts}/a_1)^2 - (\alpha_{0n}/a)^2} + \sum_{m=1}^{\infty}\sum_{n=0}^{\infty}[(C_{mn}^{+} + D_{mn}^{+})(-1)^t J_{m-t}(\alpha_{mn}\delta_1/a)\, e^{-jm\theta_0} + (C_{mn}^{-} + D_{mn}^{-})J_{m+t}(\alpha_{mn}\delta_1/a)\, e^{jm\theta_0}]\frac{\alpha_{mn}a_1/aJ_t'(\alpha_{mn}a_1/a)}{(\alpha_{ts}/a_1)^2 - (\alpha_{mn}/a)^2}. \tag{16}$$

For the two velocity boundary conditions, multiply both equations (11) and (12) by $J_t(\alpha_{ts} r/a)\,e^{jt\theta}\,dS$ and integrate equation (11) over S_1 and equation (12) over $S - S_1$, and then add these two integral equations to yield, for $t = 0$ and $s = 0$,

$$[A_{00} - B_{00}]a_1^2 = [C_{00} - D_{00}]a^2, \tag{17}$$

for $t = 0$ and $s = 1, 2, \ldots, \infty$,

$$\begin{aligned} &k[A_{00} - B_{00}]\frac{aa_1}{\alpha_{0s}} J_0(\alpha_{0s}\delta_1/a)J_1(\alpha_{0s}a_1/a) \\ &\quad - \sum_{n=1}^{\infty} k_{1,0n}[A_{0n} - B_{0n}]J_0(\alpha_{0s}\delta_1/a)\frac{\alpha_{0s}a_1/aJ_0(\alpha_{0n})J_0'(\alpha_{0s}a_1/a)}{(\alpha_{0n}/a_1)^2 - (\alpha_{0s}/a)^2} \\ &\quad - \sum_{m=1}^{\infty}\sum_{n=0}^{\infty} k_{1,mn}[(A_{mn}^+ - B_{mn}^+) + (A_{mn}^- - B_{mn}^-)] \\ &\quad \times J_m(\alpha_{0s}\delta_1/a)\frac{\alpha_{0s}a_1/aJ_m(\alpha_{mn})J_m'(\alpha_{0s}a_1/a)}{(\alpha_{mn}/a_1)^2 - (\alpha_{0s}/a)^2} \\ &= -k_{0s}[C_{0s} - D_{0s}]\frac{a^2}{2}J_0^2(\alpha_{0s}), \end{aligned} \tag{18}$$

and for $t = 1, 2, \ldots, \infty$ and $s = 0, 1, \ldots, \infty$,

$$\begin{aligned} &k[A_{00} - B_{00}]\frac{aa_1}{\alpha_{ts}} J_t(\alpha_{ts}\delta_1/a)J_1(\alpha_{ts}a_1/a) \\ &\quad - \sum_{n=1}^{\infty} k_{1,0n}[A_{0n} - B_{0n}]J_t(\alpha_{ts}\delta_1/a)\frac{\alpha_{ts}a_1/aJ_0(\alpha_{0n})J_0'(\alpha_{ts}a_1/a)}{(\alpha_{0n}/a_1)^2 - (\alpha_{ts}/a)^2} \\ &\quad - \sum_{m=1}^{\infty}\sum_{n=0}^{\infty} k_{1,mn}[(A_{mn}^+ - B_{mn}^+)J_{t+m}(\alpha_{ts}\delta_1/a) + (A_{mn}^- - B_{mn}^-)(-1)^m J_{t-m}(\alpha_{ts}\delta_1/a)] \\ &\quad \times \frac{\alpha_{ts}a_1/aJ_m(\alpha_{mn})J_m'(\alpha_{ts}a_1/a)}{(\alpha_{mn}/a_1)^2 - (\alpha_{ts}/a)^2} \\ &= -k_{ts}[C_{ts}^+ - D_{ts}^+]\frac{a^2}{2}\left(1 - \frac{t^2}{\alpha_{ts}^2}\right)J_t^2(\alpha_{ts})\,e^{-jt\theta_0}, \end{aligned} \tag{19}$$

where

$$k_{1,mn} = k[1 - (\alpha_{mn}/ka_1)^2]^{1/2}. \tag{20}$$

Similarly, multiply both equations (11) and (12) by $\mathrm{J}_t(\alpha_{ts} r/a)\,\mathrm{e}^{-\mathrm{j}t\theta}\,\mathrm{d}S$ and integrate equation (11) over S_1 and equation (12) over $S-S_1$, and then add these two integral equations to yield, for $t=1,2,\ldots,\infty$ and $s=0,1,\ldots,\infty$,

$$k[A_{00}-B_{00}]\frac{aa_1}{\alpha_{ts}}\mathrm{J}_t(\alpha_{ts}\delta_1/a)\mathrm{J}_1(\alpha_{ts}a_1/a)$$

$$-\sum_{n=1}^{\infty}k_{1,0n}[A_{0n}-B_{0n}]\mathrm{J}_t(\alpha_{ts}\delta_1/a)\frac{\alpha_{ts}a_1/a\mathrm{J}_0(\alpha_{0n})\mathrm{J}_0'(\alpha_{ts}a_1/a)}{(\alpha_{0n}/a_1)^2-(\alpha_{ts}/a)^2}$$

$$-\sum_{m=1}^{\infty}\sum_{n=0}^{\infty}k_{1,mn}[(A_{mn}^{+}-B_{mn}^{+})(-1)^m\mathrm{J}_{t-m}(\alpha_{ts}\delta_1/a)$$

$$+(A_{mn}^{-}-B_{mn}^{-})\mathrm{J}_{t+m}(\alpha_{ts}\delta_1/a)]\frac{\alpha_{ts}a_1/a\mathrm{J}_m(\alpha_{mn})\mathrm{J}_m'(\alpha_{ts}a_1/a)}{(\alpha_{mn}/a_1)^2-(\alpha_{ts}/a)^2}$$

$$=-k_{ts}[C_{ts}^{-}-D_{ts}^{-}]\frac{a^2}{2}\left(1-\frac{t^2}{\alpha_{ts}^2}\right)\mathrm{J}_t^2(\alpha_{ts})\,\mathrm{e}^{\mathrm{j}t\theta_0}. \tag{21}$$

The detailed derivation of equations (16) and (21) is given in Appendix A.

At the contraction, the boundary conditions require, for the pressure,

$$(P_C+P_D)|_{z=l}=(P_E+P_F)|_{z_2=0},\qquad (\text{on } S_2), \tag{22}$$

and, for the velocity,

$$(U_C+U_D)|_{z=l}=(U_E+U_F)|_{z_2=0},\qquad (\text{on } S_2);\qquad (U_C+U_D)|_{z=l}=0,\qquad (\text{on } S-S_2). \tag{23, 24}$$

Using the same procedure as for the expansion, equation (22) gives, for $t=0$ and $s=0$,

$$[C_{00}\,\mathrm{e}^{-\mathrm{j}kl}+D_{00}\,\mathrm{e}^{\mathrm{j}kl}]\frac{a_2^2}{2}+\sum_{n=1}^{\infty}[C_{0n}\,\mathrm{e}^{\mathrm{j}k_{0n}l}+\mathrm{D}_{0n}\,\mathrm{e}^{-\mathrm{j}k_{0n}l}]\frac{aa_2}{\alpha_{0n}}\mathrm{J}_0(\alpha_{0n}\delta_2/a)\mathrm{J}_1(\alpha_{0n}a_2/a)$$

$$+\sum_{m=1}^{\infty}\sum_{n=0}^{\infty}[(C_{mn}^{+}+C_{mn}^{-})\,\mathrm{e}^{\mathrm{j}k_{mn}l}+(D_{mn}^{+}+D_{mn}^{-})\,\mathrm{e}^{-\mathrm{j}k_{mn}l}]$$

$$\times\frac{aa_2}{\alpha_{mn}}\mathrm{J}_m(\alpha_{mn}\delta_2/a)\mathrm{J}_1(\alpha_{mn}a_2/a)=(E_{00}+F_{00})\frac{a_2^2}{2}, \tag{25}$$

for $t=0$ and $s=1,2,\ldots,\infty$,

$$\sum_{n=1}^{\infty}[C_{0n}\,\mathrm{e}^{\mathrm{j}k_{0n}l}+D_{0n}\,\mathrm{e}^{-\mathrm{j}k_{0n}l}]\mathrm{J}_0(\alpha_{0n}\delta_2/a)\frac{\alpha_{0n}a_2/a\mathrm{J}_0'(\alpha_{0n}a_2/a)}{(\alpha_{0s}/a_2)^2-(\alpha_{0n}/a)^2}$$

$$+\sum_{m=1}^{\infty}\sum_{n=0}^{\infty}[(C_{mn}^{+}+C_{mn}^{-})\,\mathrm{e}^{\mathrm{j}k_{mn}l}+(D_{mn}^{+}+D_{mn}^{-})\,\mathrm{e}^{-\mathrm{j}k_{mn}l}]\mathrm{J}_m(\alpha_{mn}\delta_2/a)$$

$$\times\frac{\alpha_{mn}a_2/a\mathrm{J}_0'(\alpha_{mn}a_2/a)}{(\alpha_{0s}/a_2)^2-(\alpha_{mn}/a)^2}=(E_{0s}+F_{0s})\frac{a_2^2}{2}\mathrm{J}_0(\alpha_{0s}), \tag{26}$$

for $t=1,2,\ldots,\infty$ and $s=0,1,\ldots,\infty$,

$$\sum_{n=1}^{\infty}[C_{0n}\,\mathrm{e}^{\mathrm{j}k_{0n}l}+D_{0n}\,\mathrm{e}^{-\mathrm{j}k_{0n}l}]\mathrm{J}_t(\alpha_{0n}\delta_2/a)\,\frac{\alpha_{0n}a_2/a\mathrm{J}_t'(\alpha_{0n}a_2/a)}{(\alpha_{ts}/a_2)^2-(\alpha_{0n}/a)^2}$$

$$+\sum_{m=1}^{\infty}\sum_{n=0}^{\infty}[(C_{mn}^{+}\,\mathrm{e}^{\mathrm{j}k_{mn}l}+D_{mn}^{+}\,\mathrm{e}^{-\mathrm{j}k_{mn}l})\mathrm{J}_{m+t}(\alpha_{mn}\delta_2/a)$$

$$+(C_{mn}^{-}\,\mathrm{e}^{\mathrm{j}k_{mn}l}+D_{mn}^{-}\,\mathrm{e}^{-\mathrm{j}k_{mn}l})(-1)^t\mathrm{J}_{m-t}(\alpha_{mn}\delta_2/a)]\,\frac{\alpha_{mn}a_2/a\mathrm{J}_t'(\alpha_{mn}a_2/a)}{(\alpha_{ts}/a_2)^2-(\alpha_{mn}/a)^2}$$

$$=(E_{ts}^{+}+F_{ts}^{+})\,\frac{a_2^2}{2}\left(1-\frac{t^2}{\alpha_{ts}^2}\right)\mathrm{J}_t(\alpha_{ts}), \tag{27}$$

and

$$\sum_{n=1}^{\infty}[C_{0n}\,\mathrm{e}^{\mathrm{j}k_{0n}l}+D_{0n}\,\mathrm{e}^{-\mathrm{j}k_{0n}l}]\mathrm{J}_t(\alpha_{0n}\delta_2/a)\,\frac{\alpha_{0n}a_2/a\mathrm{J}_t'(\alpha_{0n}a_2/a)}{(\alpha_{ts}/a_2)^2-(\alpha_{0n}/a)^2}$$

$$+\sum_{m=1}^{\infty}\sum_{n=0}^{\infty}[(C_{mn}^{+}\,\mathrm{e}^{\mathrm{j}k_{mn}l}+D_{mn}^{+}\,\mathrm{e}^{-\mathrm{j}k_{mn}l})(-1)^t\mathrm{J}_{m-t}(\alpha_{mn}\delta_2/a)$$

$$+(C_{mn}^{-}\,\mathrm{e}^{\mathrm{j}k_{mn}l}+D_{mn}^{-}\,\mathrm{e}^{-\mathrm{j}k_{mn}l})\mathrm{J}_{m+t}(\alpha_{mn}\delta_2/a)]\,\frac{\alpha_{mn}a_2/a\mathrm{J}_t'(\alpha_{mn}a_2/a)}{(\alpha_{ts}/a_2)^2-(\alpha_{mn}/a)^2}$$

$$=(E_{ts}^{-}+F_{ts}^{-})\,\frac{a_2^2}{2}\left(1-\frac{t^2}{\alpha_{ts}^2}\right)\mathrm{J}_t(\alpha_{ts}). \tag{28}$$

From the velocity boundary conditions, equations (23) and (24), for $t=0$ and $s=0$,

$$[C_{00}\,\mathrm{e}^{-\mathrm{j}kl}-D_{00}\,\mathrm{e}^{\mathrm{j}kl}]a^2=(E_{00}-F_{00})a_2^2, \tag{29}$$

for $t=0$ and $s=1,2,\ldots,\infty$,

$$k_{0s}[C_{0s}\,\mathrm{e}^{\mathrm{j}k_{0s}l}-D_{0s}\,\mathrm{e}^{-\mathrm{j}k_{0s}l}]\,\frac{a^2}{2}\,\mathrm{J}_0^2(\alpha_{0s})=-k(E_{00}-F_{00})\,\frac{aa_2}{\alpha_{0s}}\,\mathrm{J}_0(\alpha_{0s}\delta_2/a)\mathrm{J}_1(\alpha_{0s}a_2/a)$$

$$+\sum_{n=1}^{\infty}k_{2,0n}(E_{0n}-F_{0n})\mathrm{J}_0(\alpha_{0s}\delta_2/a)\,\frac{\alpha_{0s}a_2/a\mathrm{J}_0(\alpha_{0n})\mathrm{J}_0'(\alpha_{0s}a_2/a)}{(\alpha_{0n}/a_2)^2-(\alpha_{0s}/a)^2}$$

$$+\sum_{m=1}^{\infty}\sum_{n=0}^{\infty}k_{2,mn}[(E_{mn}^{+}-F_{mn}^{+})+(E_{mn}^{-}-F_{mn}^{-})]\mathrm{J}_m(\alpha_{0s}\delta_2/a)$$

$$\times\frac{\alpha_{0s}a_2/a\mathrm{J}_m(\alpha_{mn})\mathrm{J}_m'(\alpha_{0s}a_2/a)}{(\alpha_{mn}/a_2)^2-(\alpha_{0s}/a)^2}, \tag{30}$$

for $t = 1, 2, \ldots, \infty$ and $s = 0, 1, \ldots, \infty$,

$$k_{ts}[C^+_{ts}\,\mathrm{e}^{\mathrm{j}k_{ts}l} - D^+_{ts}\,\mathrm{e}^{-\mathrm{j}k_{ts}l}]\,\frac{a^2}{2}\left(1 - \frac{t^2}{\alpha^2_{ts}}\right)\mathrm{J}^2_t(\alpha_{ts}) = -k(E_{00} - F_{00})\,\frac{aa_2}{\alpha_{ts}}\,\mathrm{J}_t(\alpha_{ts}\delta_2/a)\mathrm{J}_1(\alpha_{ts}a_2/a)$$
$$+ \sum_{n=1}^{\infty} k_{2,0n}(E_{0n} - F_{0n})\mathrm{J}_t(\alpha_{ts}\delta_2/a)\,\frac{\alpha_{ts}a_2/a\,\mathrm{J}_0(\alpha_{0n})\mathrm{J}'_0(\alpha_{ts}a_2/a)}{(\alpha_{0n}/a_2)^2 - (\alpha_{ts}/a)^2}$$
$$+ \sum_{m=1}^{\infty}\sum_{n=0}^{\infty} k_{2,mn}[(E^+_{mn} - F^+_{mn})\mathrm{J}_{t+m}(\alpha_{ts}\delta_2/a) + (E^-_{mn} - F^-_{mn})(-1)^m\mathrm{J}_{t-m}(\alpha_{ts}\delta_2/a)]$$
$$\times\frac{\alpha_{ts}a_2/a\,\mathrm{J}_m(\alpha_{mn})\mathrm{J}'_m(\alpha_{ts}a_2/a)}{(\alpha_{mn}/a_2)^2 - (\alpha_{ts}/a)^2}, \tag{31}$$

and

$$k_{ts}[C^-_{ts}\,\mathrm{e}^{\mathrm{j}k_{ts}l} - D^-_{ts}\,\mathrm{e}^{-\mathrm{j}k_{ts}l}]\,\frac{a^2}{2}\left(1 - \frac{t^2}{\alpha^2_{ts}}\right)\mathrm{J}^2_t(\alpha_{ts}) = -k(E_{00} - F_{00})\,\frac{aa_2}{\alpha_{ts}}\,\mathrm{J}_t(\alpha_{ts}\delta_2/a)\mathrm{J}_1(\alpha_{ts}a_2/a)$$
$$+ \sum_{n=1}^{\infty} k_{2,0n}(E_{0n} - F_{0n})\mathrm{J}_t(\alpha_{ts}\delta_2/a)\,\frac{\alpha_{ts}a_2/a\,\mathrm{J}_0(\alpha_{0n})\mathrm{J}'_0(\alpha_{ts}a_2/a)}{(\alpha_{0n}/a_2)^2 - (\alpha_{ts}/a)^2}$$
$$+ \sum_{m=1}^{\infty}\sum_{n=0}^{\infty} k_{2,mn}[(E^+_{mn} - F^+_{mn})(-1)^m\mathrm{J}_{t-m}(\alpha_{ts}\delta_2/a) + (E^-_{mn} - F^-_{mn})\mathrm{J}_{t+m}(\alpha_{ts}\delta_2/a)]$$
$$\times\frac{\alpha_{ts}a_2/a\,\mathrm{J}_m(\alpha_{mn})\mathrm{J}'_m(\alpha_{ts}a_2/a)}{(\alpha_{mn}/a_2)^2 - (\alpha_{ts}/a)^2}, \tag{32}$$

where

$$k_{2,mn} = k[1 - (\alpha_{mn}/ka_2)^2]^{1/2}. \tag{33}$$

To determine the transmission loss of the expansion chamber, (1) the dimensions of the inlet pipe are assumed such that the incoming wave A is planar, and its magnitude A_{00} is chosen to be unity for convenience, and (2) an anechoic termination is imposed at the exit of the chamber by setting the reflected wave F to zero. Thus, equations (13)–(19), (21), and (25)–(32) give a large (theoretically infinite) number of relations $4(2t+1)(s+1)$ for a large number of unknowns $4(2m+1)(n+1)$. The unknowns are the pressure magnitudes for incident and reflected waves in the inlet duct, the chamber, and outlet duct (B_{mn}, C_{mn}, D_{mn} and E_{mn}). Since higher modes have a diminishing effect on the solution, t and m can be truncated to p and s and n to q resulting in $4(2p+1)(q+1)$ equations with $4(2p+1)(q+1)$ unknowns. The values of p and q needed for a converged solution depend on the magnitude of the area transition, the length of the chamber, and the frequency range of interest. For the geometries and frequencies investigated here (see Figure 1 and the companion paper [15]), $p = 5$ and $q = 5$ were found to be sufficient. Once equations (13)–(19), (21), and (25)–(32) are solved, the transmission loss is determined in the centre of the duct by

$$TL = -20\log_{10}\left\{(a_2/a_1)\left|E_{00}\,\mathrm{e}^{-\mathrm{j}kl_2} + \sum_{n=1}^{q} E_{0n}\,\mathrm{e}^{\mathrm{j}k_{2,0n}l_2}\right|\right\}. \tag{34}$$

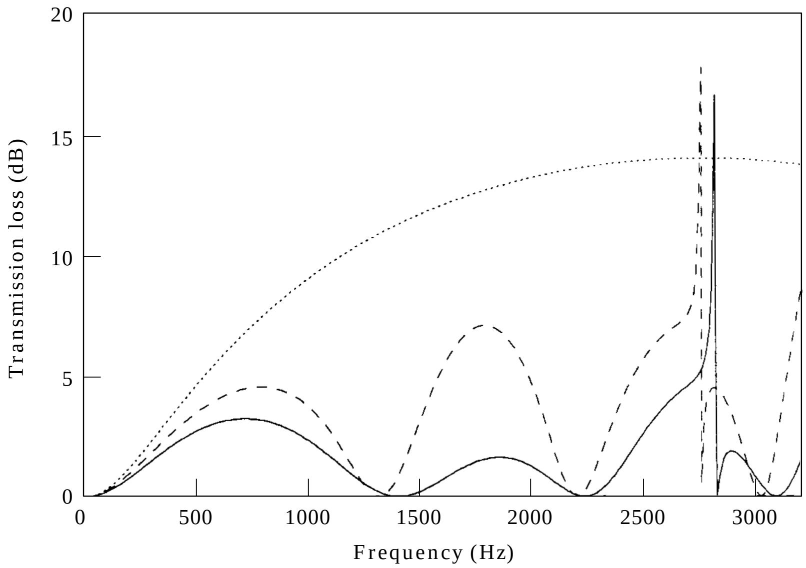

Figure 2. Transmission loss of circular expansion chamber with $l/d = 0{\cdot}205$, $\delta_1 = \delta_2 = 5{\cdot}10$ cm and $\theta_0 = 180°$: ——, analytical, present (chamber and end ducts); · · · · · , one-dimensional; – – –, analytical, Ih and Lee (chamber only).

Note that the non-propagating modes leaving the expansion chamber in the outlet duct will decay rapidly over the short distance l_2 due to the smaller duct diameter. This distance is chosen so that the higher modes will have a negligible effect on the transmission loss calculations.

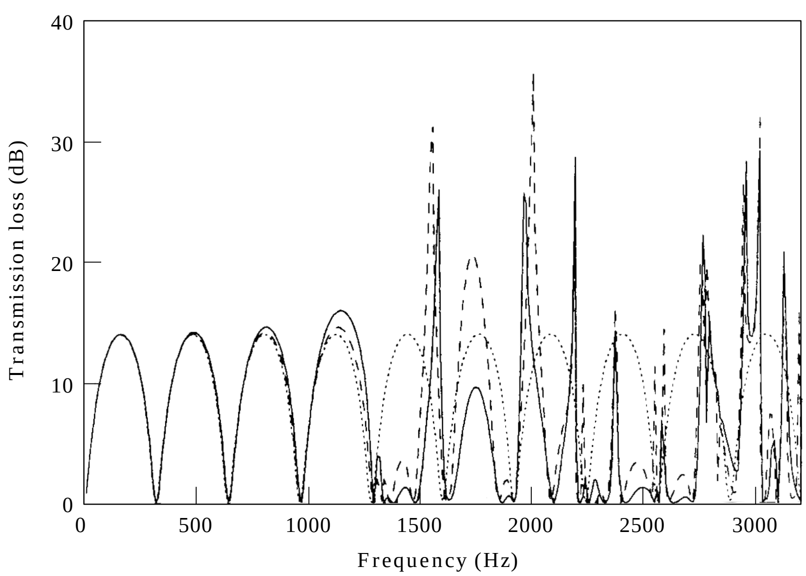

Figure 3. Transmission loss of circular expansion chamber with $l/d = 3{\cdot}525$, $\delta_1 = \delta_2 = 5{\cdot}10$ cm and $\theta_0 = 180°$: ——, analytical, present (chamber and end ducts); · · · · · , one-dimensional; – – –, analytical, Ih and Lee (chamber only).

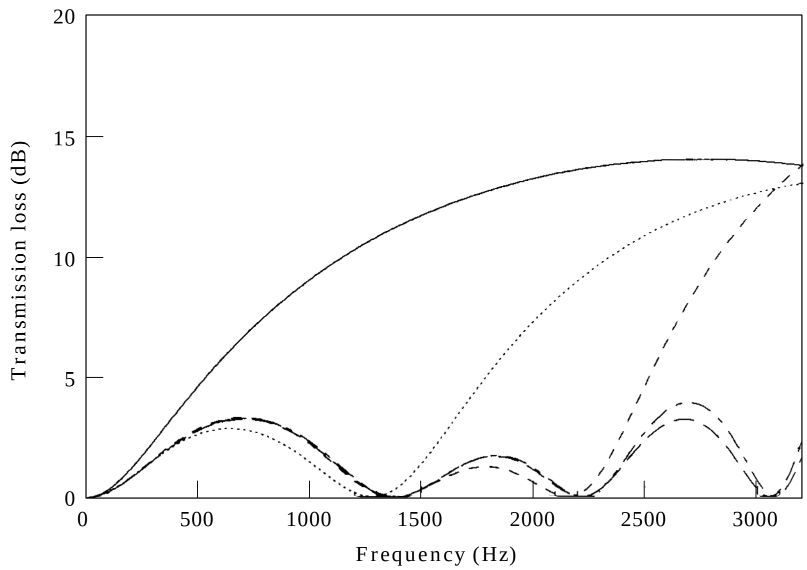

Figure 4. The effect of p-terms on transmission loss of circular expansion chamber with $l/d = 0{\cdot}205$, $\delta_1 = \delta_2 = 5{\cdot}10$ cm and $\theta_0 = 180°$: ——, $p=0$, $q=0$; · · · · ·, $p=1$, $q=0$; – – –, $p=2$, $q=0$; — — —, $p=3$, $q=0$; — · — ·, $p=4$, $q=0$.

Setting $p = 0$ and $q = 0$ in equations (13), (17), (25) and (29) yields the classical transmission loss of a one-dimensional expansion chamber as, for $a_1 = a_2$,

$$TL = 10 \log_{10}\left[1 + \frac{1}{4}\left(m - \frac{1}{m}\right)^2 \sin^2 kl\right]. \tag{35}$$

The foregoing formulation allows θ_0 to vary between 0 and 180°. An extensive experimental and computational work was conducted to validate the formulation presented here. While the detailed comparisons among the analytical development and the experimental study and the boundary element predictions are described and discussed in a companion paper [15], two extreme configurations are considered next for illustration purposes.

3. RESULTS AND DISCUSSION

Consider expansion chambers of $l/d = 0{\cdot}205$ and $l/d = 3{\cdot}525$ with the relative offset angle $\theta_0 = 180°$ (see Figure 1 for the remaining dimensions). Figures 2 and 3 show illustrative comparisons of transmission loss results from the present three-dimensional approach ($p = 5, q = 5$) and the one-dimensional theory for $l/d = 0{\cdot}205$ and $3{\cdot}525$, respectively. The short expansion chamber of Figure 2 clearly shows no similarity between the one-dimensional results and the three-dimensional predictions of the present approach. For the long expansion chamber, a good agreement is shown in Figure 3 at low frequencies, whereas at higher frequencies noticeable magnitude differences are observed before the complete breakdown of the repeating one-dimensional domes. Thus, the higher order modes can decay sufficiently in the long chamber leading to axially one-dimensional propagation at low frequencies. With increasing frequency, however, additional modes are excited at the area discontinuities and do not decay completely. Non-planar effects then

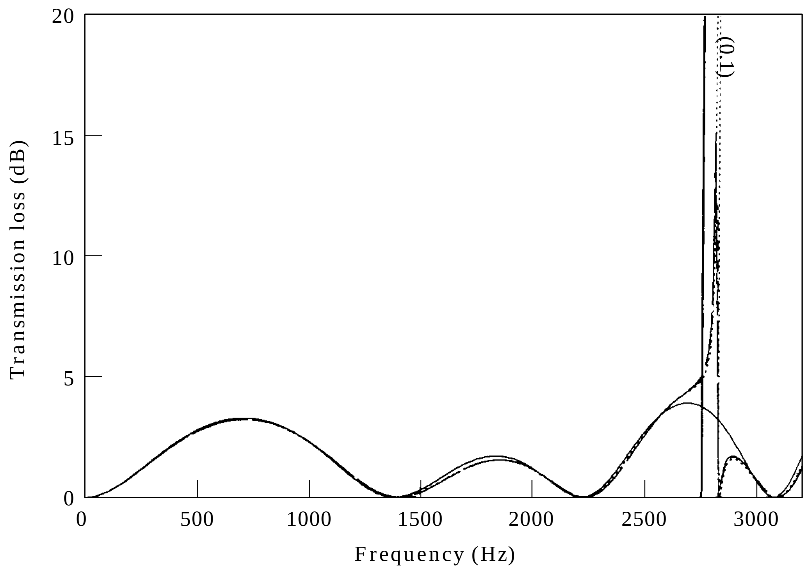

Figure 5. The effect of q-terms on transmission loss of circular expansion chamber with $l/d = 0{\cdot}205$, $\delta_1 = \delta_2 = 5{\cdot}10$ cm and $\theta_0 = 180°$: ——, $p=4$, $q=0$; · · · · · , $p=4$, $q=1$; – – –, $p=4$, $q=2$; — —, $p=4$, $q=3$.

spread throughout the length of the chamber and influence the acoustic attenuation performance.

Also included in Figures 2 and 3 are the transmission loss results from Ih and Lee's analytical approach, which chose not to include the end ducts and used cross-sectional averages on the inlet and outlet ports of the chamber. Thus, the differences between the present predictions and Ih and Lee's approach may become pronounced for the short-length expansion chamber (note, for example, the second attenuation band in Figure 2). Figure 2 for the short expansion chamber illustrates the importance of the exponential decay of the non-planar wave effects in the inlet and outlet ducts on the transmission loss performance. Due to the very short chamber length, higher order modes excited at the inlet discontinuity do not have a sufficient length to decay in the expansion chamber. Some modes pass through the chamber and combine with the higher order modes excited at the outlet discontinuity, which gives the outlet duct a large multidimensional component. These modes passed on to the exit duct will then decay quickly in the much smaller outlet diameter, resulting in essentially planar wave propagation in a short distance. This fact provided the motivation for this study to develop an analytical approach which combines multidimensional wave propagation in the chamber with the two offset end ducts. The differences become less pronounced with increasing length of the expansion chamber, since most higher order modes excited at the inlet decay over the longer chamber length before reaching the outlet (see Figure 3).

El-Sharkawy and Nayfeh [3] reported for their configuration that five terms of Bessel function expansion were sufficient to converge to 0·1% accuracy. Figures 4 and 5 demonstrate the contribution from individual terms for the short chamber of Figure 2. Within the frequency range considered here, five terms also appear to be sufficient for the convergence in terms of p (Figure 4). While $p = q = 5$ is used in the present study uniformly to ensure accuracy, it is interesting to note that combining the five terms of Figure 4 with only one additional term in q, that is $p = 4$, $q = 1$, would yield a reasonable final prediction.

4. CONCLUDING REMARKS

A three-dimensional analytical approach has been developed to predict the acoustic attenuation performance of the circular expansion chamber with offset inlet/outlet. The analytical approach provides expressions for the acoustic pressure and velocity in the chamber and the attached ducts. These results may then be used to determine transmission loss and four-pole parameters. While the former is used in the present study, the latter can also be evaluated by following an approach similar to that of Sahasrabudhe *et al*. [17, 18]. The effect of inlet and outlet ducts on transmission loss is illustrated by comparing the present predictions with the ducts attached to those with the ducts removed (simple openings). For particularly short expansion chambers, the effect of end ducts is found to be pronounced due to the decaying higher order modes in the inlet and outlet ducts. It is this effect that led to the development of a three-dimensional analytical approach of the present study to couple wave propagation in the chamber with the two end ducts. Since the Mach number in expansion chambers is usually low in numerous applications, the convective effect of mean flow on the acoustic attenuation is negligible (see, for example, Ji and Sha [19]), therefore excluded from the present work. An extensive experimental and computational validation effort is presented in a companion paper [15].

REFERENCES

1. D. D. Davis, G. M. Stokes, D. Moore and G. L. Stevens 1954 *NACA TN* 1192. Theoretical and experimental investigations of mufflers with comments on engine exhaust muffler design.
2. J. Miles 1944 *Journal of the Acoustical Society of America* **16**, 14–19. The reflection of sound due to a change in cross section of a circular tube.
3. A. I. El-Sharkawy and A. H. Nayfeh 1978 *Journal of the Acoustical Society of America* **63**, 667–674. Effect of the expansion chamber on the propagation of sound in circular pipes.
4. M. Åbom 1990 *Journal of Sound and Vibration* **137**, 403–418. Derivation of four-pole parameters including higher order mode effects for expansion chamber mufflers with extended inlet and outlet.
5. A. Selamet and P. M. Radavich 1997 *Journal of Sound and Vibration* **201**, 407–426. The effect of length on the acoustic attenuation performance of concentric expansion chambers: an analytical, computational, and experimental investigation.
6. L. J. Eriksson 1980 *Journal of the Acoustical Society of America* **68**, 545–550. Higher order mode effects in the circular ducts and expansion chambers.
7. L. J. Eriksson 1982 *Journal of the Acoustical Society of America* **72**, 1208–1211. Effect of inlet/outlet locations on higher order modes in silencers.
8. L. J. Eriksson, C. A. Anderson, R. H. Hoops and K. Jayaraman 1983 *Proceedings of* 11*th ICA*, *Paris*, 329–332. Finite length effects on higher order mode propagation in silencers.
9. J. G. Ih and B. H. Lee 1985 *Journal of the Acoustical Society of America* **77**, 1377–1388. Analysis of higher-order mode effects in the circular expansion chamber with mean flow.
10. S. I. Yi and B. H. Lee 1986 *Journal of the Acoustical Society of America* **79**, 1299–1306. Three-dimensional acoustic analysis of circular expansion chambers with a side inlet and a side outlet.
11. S. I. Yi and B. H. Lee 1987 *Journal of the Acoustical Society of America* **81**, 1279–1287. Three-dimensional acoustic analysis of a circular expansion chamber with side inlet and end outlet.
12. J. Kim and W. Soedel 1989 *Journal of Sound and Vibration* **129**, 237–254. General formulation of four pole parameters for three-dimensional cavities utilizing modal expansion, with special attenuation to the annular cylinder.
13. P. C.-C. Lai and W. Soedel 1996 *Journal of Sound and Vibration* **194**, 137–171. Two dimensional analysis of thin, shell or plate like muffler elements.
14. A. Selamet, Z. L. Ji and P. M. Radavich 1997 *ASME International Congress and Exposition–Noise Control and Acoustics Division*, *Dallas*, *TX* (T. M. Farabee *et al*., editors) NCA-Vol. 24, 285–290. Circular expansion chambers with offset inlet/outlet.

15. A. SELAMET, Z. L. JI and P. M. RADAVICH 1998 *Journal of Sound and Vibration* **213,** 619–641. Acoustic attenuation performance of circular expansion chambers with offset inlet/outlet: II. Comparison with experimental and computational studies.
16. M. L. MUNJAL 1987 *Acoustics of Ducts and Mufflers*. New York: Wiley-Interscience.
17. A. D. SAHASRABUDHE, S. A. RAMU and M. L. MUNJAL 1991 *Journal of Sound and Vibration* **147**, 371–394. Matrix condensation and transfer matrix techniques in the 3-D analysis of expansion chamber mufflers.
18. A. D. SAHASRABUDHE and M. L. MUNJAL 1995 *Journal of Sound and Vibration* **185**, 515–529. Analysis of inertance due to the higher order mode effects in a sudden area discontinuity.
19. Z. L. JI and J. Z. SHA 1995 *Journal of the Acoustical Society of America* **98**, 2848–2850. Four-pole parameters of a duct with low Mach number flow.
20. C. J. TRANTER 1969 *Bessel Functions with Some Physical Applications*. New York: Hart Publishing Co.

APPENDIX A: DERIVATION OF EQUATIONS (16) AND (21)

For the pressure boundary condition, multiply both sides of equation (10) by $J_t(\alpha_{ts} r_1/a_1)\,e^{-jt\varphi}\,dS$, and integrate over S_1 to get

$$\begin{aligned}
&\int_0^{2\pi}\int_0^{a_1}\Bigg\{[A_{00}+B_{00}]+\sum_{n=1}^{\infty}[A_{0n}+B_{0n}]J_0(\alpha_{0n}r_1/a_1)\\
&\qquad+\sum_{m=1}^{\infty}\sum_{n=0}^{\infty}[(A^+_{mn}+B^+_{mn})\,e^{-jm\varphi}+(A^-_{mn}+B^-_{mn})\,e^{jm\varphi}]J_m(\alpha_{mn}r_1/a_1)\Bigg\}\\
&\qquad\times J_t(\alpha_{ts}r_1/a_1)\,e^{-jt\varphi}r_1\,dr_1\,d\varphi\\
&\quad=\int_0^{2\pi}\int_0^{a_1}\Bigg\{[C_{00}+D_{00}]+\sum_{n=1}^{\infty}[C_{0n}+D_{0n}]J_0(\alpha_{0n}r/a)\\
&\qquad+\sum_{m=1}^{\infty}\sum_{n=0}^{\infty}[(C^+_{mn}+D^+_{mn})\,e^{-jm\theta}+(C^-_{mn}+D^-_{mn})\,e^{jm\theta}]J_m(\alpha_{mn}r/a)\Bigg\}\\
&\qquad\times J_t(\alpha_{ts}r_1/a_1)\,e^{-jt\varphi}r_1\,dr_1\,d\varphi.
\end{aligned}\tag{A1}$$

Using Graf's addition theorem for Bessel functions [20],

$$J_m(\mu r)\,e^{-jm\theta}=\sum_{P=-\infty}^{\infty}J_{m+P}(\mu\delta_1)J_P(\mu r_1)\,e^{-j(P\varphi+m\theta_0)},\tag{A2}$$

for the right side of equation (A1) to transform the co-ordinates of chamber to those of the inlet duct, and then integrating over φ from 0 to 2π for both sides yields

$$\begin{aligned}
&\int_0^{a_1}\sum_{n=0}^{\infty}[A^-_{tn}+B^-_{tn}]J_t(\alpha_{tn}r_1/a_1)J_t(\lambda_{ts}r_1/a_1)r_1\,dr_1\\
&\quad=\int_0^{a_1}\Bigg\{\sum_{n=1}^{\infty}[C_{0n}+D_{0n}]J_t(\alpha_{0n}\delta_1/a)J_t(\alpha_{0n}r_1/a)\\
&\qquad+\sum_{m=1}^{\infty}\sum_{n=0}^{\infty}[(C^+_{mn}+D^+_{mn})(-1)^tJ_{m-t}(\alpha_{mn}\delta_1/a)\,e^{-jm\theta_0}\\
&\qquad+(C^-_{mn}+D^-_{mn})J_{m+t}(\alpha_{mn}\delta_1/a)\,e^{jm\theta_0}]J_t(\alpha_{mn}r_1/a)\Bigg\}J_t(\alpha_{ts}r_1/a_1)r_1\,dr_1.
\end{aligned}\tag{A3}$$

Integrating over r_1 from 0 to a_1, using the integral relations of Bessel functions [20]

$$\int r\mathrm{J}_m(\lambda r)\mathrm{J}_m(\mu r)\,\mathrm{d}r = \begin{cases} \dfrac{r}{\lambda^2-\mu^2}\{\mu\mathrm{J}_m(\lambda r)\mathrm{J}'_m(\mu r) - \lambda\mathrm{J}_m(\mu r)\mathrm{J}'_m(\lambda r)\} & (\lambda \neq \mu) \\ \dfrac{r^2}{2}\left\{[\mathrm{J}'_m(\lambda r)]^2 + \left[1-\dfrac{m^2}{\lambda^2 r^2}\right]\mathrm{J}_m^2(\lambda r)\right\} & (\lambda = \mu) \end{cases}, \tag{A4}$$

and applying equation (4) for the radial boundary condition gives

$$\begin{aligned}[A_{ts}^- + B_{ts}^-]\frac{a_1^2}{2}\left(1-\frac{t^2}{\alpha_{ts}^2}\right)\mathrm{J}_t(\alpha_{ts}) = {} & \sum_{n=1}^{\infty}[C_{0n}+D_{0n}]\mathrm{J}_t(\alpha_{0n}\delta_1/a)\frac{\alpha_{0n}a_1/a\mathrm{J}'_t(\alpha_{0n}a_1/a)}{(\alpha_{ts}/a_1)^2-(\alpha_{0n}/a)^2} \\ & + \sum_{m=1}^{\infty}\sum_{n=0}^{\infty}[(C_{mn}^+ + D_{mn}^+)(-1)^t\mathrm{J}_{m-t}(\alpha_{mn}\delta_1/a)\,\mathrm{e}^{-\mathrm{j}m\theta_0} \\ & + (C_{mn}^- + D_{mn}^-)\mathrm{J}_{m+t}(\alpha_{mn}\delta_1/a)\,\mathrm{e}^{\mathrm{j}m\theta_0}]\frac{\alpha_{mn}a_1/a\mathrm{J}'_t(\alpha_{mn}a_1/a)}{(\alpha_{ts}/a_1)^2-(\alpha_{mn}/a)^2}\end{aligned} \tag{A5}$$

which is identical to equation (16).

For the velocity boundary conditions, multiply both sides of equations (11) and (12) by $\mathrm{J}_t(\alpha_{ts}r/a)\,\mathrm{e}^{-\mathrm{j}t\theta}\,\mathrm{d}S$ and integrate equation (11) over S_1 and equation (12) over $S-S_1$, and then add these two integral equations to get

$$\begin{aligned}&\int_0^{2\pi}\int_0^{a_1}\Bigg\{k[A_{00}-B_{00}] - \sum_{n=1}^{\infty}k_{1,0n}[A_{0n}-B_{0n}]\mathrm{J}_0(\alpha_{0n}r_1/a_1) \\ &\quad - \sum_{m=1}^{\infty}\sum_{n=0}^{\infty}k_{1,mn}[(A_{mn}^+ - B_{mn}^+)\,\mathrm{e}^{-\mathrm{j}m\varphi} + (A_{mn}^- - B_{mn}^-)\,\mathrm{e}^{\mathrm{j}m\varphi})]\mathrm{J}_m(\alpha_{mn}r_1/a_1)\Bigg\} \\ &\quad \times \mathrm{J}_t(\alpha_{ts}r/a)\,\mathrm{e}^{-\mathrm{j}t\theta}r_1\,\mathrm{d}r_1\,\mathrm{d}\varphi = \int_0^{2\pi}\int_0^{a}\{k[C_{00}-D_{00}] - \sum_{n=1}^{\infty}k_{0n}[C_{0n}-D_{0n}]\mathrm{J}_0(\alpha_{0n}r/a) \\ &\quad - \sum_{m=1}^{\infty}\sum_{n=0}^{\infty}k_{mn}[(C_{mn}^+ - D_{mn}^+)\,\mathrm{e}^{-\mathrm{j}m\theta} + (C_{mn}^- - D_{mn}^-)\,\mathrm{e}^{\mathrm{j}m\theta}]\mathrm{J}_m(a_{mn}r/a)\Bigg\} \\ &\quad \times \mathrm{J}_t(a_{ts}r/a)\,\mathrm{e}^{-\mathrm{j}t\theta}r\,\mathrm{d}r\,\mathrm{d}\theta.\end{aligned} \tag{A6}$$

Using Graf's addition theorem for Bessel functions (A2) for the left side of equation (A6) to transform the co-ordinates of the chamber to those of the inlet duct, and then integrating over φ for the left side and over θ for the right side, yields

$$\begin{aligned}&\int_0^{a_1}\Bigg\{k[A_{00}-B_{00}]\mathrm{J}_t(\alpha_{ts}\delta_1/a)\mathrm{J}_0(\alpha_{ts}r_1/a) \\ &\quad - \sum_{n=1}^{\infty}k_{1,0n}[A_{0n}-B_{0n}]\mathrm{J}_0(\alpha_{0n}r_1/a_1)\mathrm{J}_t(\alpha_{ts}\delta_1/a)\mathrm{J}_0(\alpha_{ts}r_1/a)\end{aligned}$$

$$- \sum_{m=1}^{\infty} \sum_{n=0}^{\infty} k_{1,mn} [(A_{mn}^{+} - B_{mn}^{+})(-1)^m \mathrm{J}_{t-m}(\alpha_{ts}\delta_1/a) + (A_{mn}^{-} - B_{mn}^{-})\mathrm{J}_{t+m}(\alpha_{ts}\delta_1/a)]$$

$$\left. \times \mathrm{J}_m(\alpha_{mn} r_1/a_1)\mathrm{J}_m(\alpha_{ts} r_1/a) \right\} \mathrm{e}^{-\mathrm{j}t\theta_0} r_1 \, \mathrm{d}r_1$$

$$= -\int_0^a \sum_{n=0}^{\infty} k_{tn} [C_{tn}^{-} - D_{tn}^{-}] \mathrm{J}_t(\alpha_{tn} r/a)\mathrm{J}_t(\alpha_{ts} r/a) r \, \mathrm{d}r. \tag{A7}$$

Integrating r_1 and r for the left and right sides of equation (A7), and using the integral relation (A4) for Bessel functions, yields

$$k[A_{00} - B_{00}] \frac{aa_1}{\alpha_{ts}} \mathrm{J}_t(\alpha_{ts}\delta_1/a)\mathrm{J}_1(\alpha_{ts}a_1/a) - \sum_{n=1}^{\infty} k_{1,0n}[A_{0n} - B_{0n}]\mathrm{J}_t(\alpha_{ts}\delta_1/a)$$

$$\times \frac{\alpha_{ts} a_1/a \mathrm{J}_0(\alpha_{0n})\mathrm{J}_0'(\alpha_{ts}a_1/a)}{(\alpha_{0n}/a_1)^2 - (\alpha_{ts}/a)^2} - \sum_{m=1}^{\infty} \sum_{n=0}^{\infty} k_{1,mn}[(A_{mn}^{+} - B_{mn}^{+})(-1)^m \mathrm{J}_{t-m}(\alpha_{ts}\delta_1/a)$$

$$+ (A_{mn}^{-} - B_{mn}^{-})\mathrm{J}_{t+m}(\alpha_{ts}\delta_1/a)] \frac{\alpha_{ts} a_1/a \mathrm{J}_m(\alpha_{mn})\mathrm{J}_m'(\alpha_{ts}a_1/a)}{(\alpha_{mn}/a_1)^2 - (\alpha_{ts}/a)^2}$$

$$= -k_{ts}[C_{ts}^{-} - D_{ts}^{-}] \frac{a^2}{2}\left(1 - \frac{t^2}{\alpha_{ts}^2}\right) \mathrm{J}_t^2(\alpha_{ts}\} \mathrm{e}^{\mathrm{j}t\theta_0} \tag{A8}$$

which is identical to equation (21).

APPENDIX B: NOMENCLATURE

a, a_1, a_2	radii of expansion chamber, inlet and outlet ducts
A, B, C, D, E, F	pressure coefficients
c	speed of sound
f	frequency
j	$= \sqrt{-1}$, imaginary unit
$\mathrm{J}_m(x)$	Bessel function of the first kind of order m
k	planar wavenumber
$k_{mn}, k_{l,mn}, k_{2,mn}$	axial wavenumbers in expansion chamber, inlet and outlet ducts
l	length of expansion chamber
m	asymmetric mode number, expansion ratio
n	radial mode number
p	number of m-terms after truncation
P	acoustic pressure
q	number of n-terms after truncation
(r, θ, z)	cylindrical co-ordinate system for chamber
(r_1, φ, z_1)	cylindrical co-ordinate system for inlet pipe
(r_2, φ, z_2)	cylindrical co-ordinate system for outlet pipe
s	orthogonal expansion terms
S, S_1, S_2	cross-sectional areas of expansion chamber, inlet and outlet ducts
t	orthogonal expansion terms

TL	transmission loss
U	particle velocity
α_{mn}	zeros of $J_m(\alpha_{mn}) = 0$
δ_1, δ_2	inlet and outlet offset distances from the centre of expansion chamber
θ_0	relative angle between inlet and outlet
ρ	medium density
ω	angular frequency